



Stabilization of higher- κ tetragonal Hf O 2 by Si O 2 admixture enabling thermally stable metal-insulator-metal capacitors

T. S. Böске, S. Govindarajan, P. D. Kirsch, P. Y. Hung, C. Krug, B. H. Lee, J. Heitmann, U. Schröder, G. Pant, B. E. Gnade, and W. H. Krautschneider

Citation: *Applied Physics Letters* **91**, 072902 (2007); doi: 10.1063/1.2771376

View online: <http://dx.doi.org/10.1063/1.2771376>

View Table of Contents: <http://scitation.aip.org/content/aip/journal/apl/91/7?ver=pdfcov>

Published by the [AIP Publishing](#)

Articles you may be interested in

[High capacitance density metal-insulator-metal structures based on a high- \$\kappa\$ Hf N x O y – Si O 2 – Hf Ti O y laminate stack](#)

Appl. Phys. Lett. **92**, 132902 (2008); 10.1063/1.2905273

[Electric-field-driven dielectric breakdown of metal-insulator-metal hafnium silicate](#)

Appl. Phys. Lett. **91**, 243514 (2007); 10.1063/1.2825288

[High-temperature conduction behaviors of HfO 2 / TaN -based metal-insulator-metal capacitors](#)

J. Appl. Phys. **102**, 073706 (2007); 10.1063/1.2786712

[Atomic-layer-deposited Al 2 O 3 – Hf O 2 – Al 2 O 3 dielectrics for metal-insulator-metal capacitor applications](#)

Appl. Phys. Lett. **87**, 053501 (2005); 10.1063/1.2005397

[Physical and electrical characterization of HfO 2 metal-insulator-metal capacitors for Si analog circuit applications](#)

J. Appl. Phys. **94**, 551 (2003); 10.1063/1.1579550

The image shows the cover of an Applied Physics Reviews journal. It features a blue and orange color scheme with a molecular structure background. The text 'NEW Special Topic Sections' is prominently displayed in white. Below it, 'NOW ONLINE' is written in orange, followed by 'Lithium Niobate Properties and Applications: Reviews of Emerging Trends' in white. The AIP Applied Physics Reviews logo is in the bottom right corner.

NEW Special Topic Sections

NOW ONLINE
Lithium Niobate Properties and Applications:
Reviews of Emerging Trends

AIP Applied Physics
Reviews

Stabilization of higher- κ tetragonal HfO₂ by SiO₂ admixture enabling thermally stable metal-insulator-metal capacitors

T. S. Böske,^{a)} S. Govindarajan,^{b)} P. D. Kirsch, P. Y. Hung, C. Krug,^{c)} and B. H. Lee
SEMATECH, 2706 Montopolis Dr., Austin, Texas, 78741

J. Heitmann and U. Schröder
Qimonda Dresden GmbH & Co. OHG, Königsbrücker Str. 180, 01099 Dresden, Germany

G. Pant and B. E. Gnade
Department of Electrical Engineering, University of Texas at Dallas, Richardson, Texas 75080

W. H. Krautschneider
Technical University of Hamburg-Harburg, Department of Nanoelectronics, 21071 Hamburg, Germany

(Received 19 March 2007; accepted 24 July 2007; published online 14 August 2007)

The authors report the relationship between HfO₂ crystalline phase and the resulting electrical properties. Crystallization of amorphous HfO₂ into the monoclinic phase led to a significant increase in leakage current and formation of local defects. Admixture of 10% SiO₂ avoided formation of these defects by stabilization of the tetragonal phase, and concurrently increased the permittivity to 35. This understanding enabled fabrication of crystalline HfO₂ based metal-insulator-metal capacitors able to withstand a thermal budget of 1000 °C while optimizing capacitance equivalent thickness (<1.3 nm) at low leakage [$J(1\text{ V}) < 10^{-7}\text{ A/cm}^2$]. © 2007 American Institute of Physics. [DOI: 10.1063/1.2771376]

Hafnium based oxides are currently leading candidates for high- k dielectrics in gate insulators and dynamic random access memory (DRAM) capacitors. A well known issue is the existence of intrinsic traps in the crystalline phases of HfO₂.^{1,2} Material engineering for practical applications of HfO₂ has therefore mainly concentrated on preventing crystallization. Two common approaches are reducing the thermal budget, as applied in stack capacitor DRAM,³ and reducing the film thickness in transistors.⁴ However, dielectrics for deep trench DRAM capacitors⁵ have to withstand a high thermal budget above 1000 °C because the capacitor is processed before array transistor formation. At the same time, a relatively thick dielectric is required to meet the leakage current specification (10^{-8} – 10^{-7} A/cm^2 at 1 V). Since thicker films of HfO₂ crystallize more easily,⁶ crystallization of a hafnium rich dielectric cannot be prevented in this application. Hence, optimization of the crystalline state is crucial.

When hafnium oxide is deposited at low temperature by an atomic layer deposition (ALD) process, it remains amorphous. Crystallization in bulk films occurs above 350 °C. When the film thickness is reduced, the crystallization temperature increases. Crystalline HfO₂ exists in the monoclinic phase at normal pressure and temperatures below 1700 °C, while a transformation into the tetragonal phase takes place at higher temperatures. However, when the crystal size is reduced to the nanometer range, increased stability of the tetragonal phase is observed even at lower temperatures due to a surface energy effect.⁷ Crystallization in thin films does usually proceed by nucleation in the tetragonal phase due to this, and a subsequent transformation of the crystallites to the monoclinic phase appears during growth and cooling. The

stability of the tetragonal phase can be increased by adding suitable dopants,⁸ until complete stabilization at room temperature is achieved in thin films. A benefit of tetragonal films is an increased dielectric constant; that of monoclinic phase is 16–18, while a value between 28.5 (Ref. 9) and 70 (Ref. 10) is predicted for the tetragonal phase. Previous experimental studies of phase stabilization^{11–13} concentrated on the dielectric constant alone. In this letter, we report the relationship between HfO₂ crystallization, leakage current, and dielectric constant and apply this understanding to improve dielectric scaling at technologically relevant thermal budget and film thickness.

HfO₂ and HfSiO_x films were deposited by an ALD process using tetrakis(ethylmethylamino)hafnium, tetrakis(ethylmethylamino)silicon, and ozone. Si content of the films was controlled by varying flow rates of the precursors.¹⁴ The composition was monitored by Rutherford backscattering and x-ray photoelectron spectroscopy (XPS). Blanket films for physical characterization were deposited on TiN and subsequently annealed in N₂ at the given temperature. Integrity of the stack and absence of intermixing of HfSiO_x and

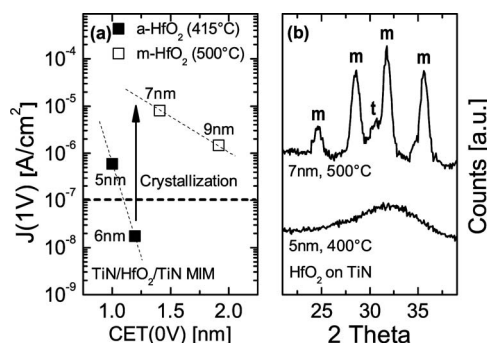


FIG. 1. (a) Leakage current vs CET relation for HfO₂ MIM capacitors with slight variation in thermal budget. (b) X-ray diffraction spectra suggesting crystallization of HfO₂ as source of leakage current degradation.

^{a)}Present address: Qimonda Dresden, Germany; electronic mail: tim.boescke@qimonda.com

^{b)}Present address: Qimonda Richmond.

^{c)}Present address: Universidade Federal do Rio Grande do Sul, Brazil.

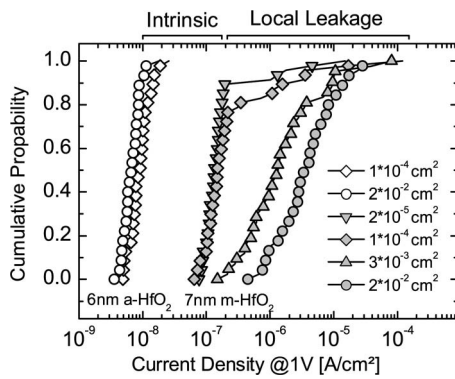


FIG. 2. Area statistics of leakage current density for amorphous and monoclinic HfO_2 . Strong area dependence for crystalline HfO_2 suggests both an intrinsic and extrinsic (local defects) contribution.

TiN after high temperature steps was confirmed by transmission electron microscopy and XPS. The film thickness was measured using x-ray reflectometry. Crystallinity and phase composition were determined by grazing incidence x-ray diffraction (XRD) and selective area electron diffraction. Dielectric constants were determined from the capacitance density of the dielectric on top of TiN measured by a contactless corona charge method. All further electrical characterizations were performed on metal-insulator-metal (MIM) capacitors with ALD TiN electrodes. Devices with an area of 1×10^{-4} and 2×10^{-2} cm^2 were used for capacitance and leakage current measurements, respectively, unless noted differently.

Figure 1(a) shows the relation between leakage current and capacitance equivalent thickness (CET) for MIM capacitors with undoped HfO_2 . Films below 7 nm thickness stay amorphous at a total thermal budget of 415 °C, as confirmed by XRD [Fig. 1(b)]. Low leakage is observed for these samples. However, an increase in thickness and thermal budget, to 7 nm and 500 °C, respectively, leads to a significant degradation of the leakage current. XRD confirms that the degradation is coincident with crystallization into a predominantly monoclinic phase, with a small fraction ($\approx 10\%$) of tetragonal HfO_2 . Further insight is gained from device area statistics (Fig. 2). While the leakage current density of amorphous films is independent of area and uniform across the wafer, significant nonuniformity and area dependence are observed for crystallized HfO_2 . The distribution resembles a Poisson statistic, which suggests a random area distribution of local defects with high leakage. For devices with an area of 1×10^{-4} cm^2 and below, the probability to contain a defect is smaller than 1 so that only a fraction of the devices shows increased leakage, while one or more defects are likely for larger devices.

The leakage increase can be separated into an intrinsic (area independent) and an extrinsic (local defects) contribution. We attribute the intrinsic degradation to the generation of shallow electron traps, leading to an increase of trap assisted leakage current.¹⁵ A potential root cause is the existence of oxygen vacancies¹ in the crystalline phase. The origin of the extrinsic defects may be of mechanical nature. The presence of residual $t\text{-HfO}_2$ [Fig. 3(b)] implies that a tetragonal to monoclinic transformation took place during the crystallization. The phase transformation leads to local compressive and shear stress due to volume increase and change of crystal symmetries,¹⁶ which can be unloaded by microcracks and roughening of the surface. Physical evidence for

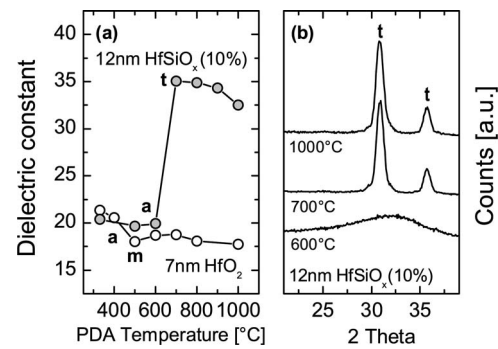


FIG. 3. (a) Evolution of dielectric constant with annealing temperature for HfO_2 and $\text{Hf}_{0.9}\text{Si}_{0.1}\text{O}_2$. (b) X-ray diffraction indicates crystallization into the tetragonal phase for $\text{Hf}_{0.9}\text{Si}_{0.1}\text{O}_2$.

this effect in HfO_2 thin films has been reported.¹⁷

The transformation into the monoclinic phase can be avoided by stabilizing the tetragonal phase. Remarkably, this can be achieved with a dopant as common as silicon oxide.^{11,18,19} We previously determined that a minimum of 10% SiO_2 addition is required to stabilize the tetragonal phase completely and also the dielectric constant is optimized at this point.²⁰ Figure 3(a) compares the evolution of dielectric constants of HfO_2 and $\text{Hf}_{0.9}\text{Si}_{0.1}\text{O}_2$ after different annealings. The dielectric constant of the amorphous phase is slightly above 20 for both films. The dielectric constant of pure HfO_2 reduces to 18 when crystallizing into the monoclinic phase at 500 °C. The admixture of silicon increases the crystallization temperature of HfO_2 . XRD [Fig. 3(b)] indicates crystallization into a high symmetry phase above 700 °C. Distinguishing between the cubic and tetragonal phases by XRD in thin films is difficult due to limited sensitivity and resolution. However, selective area electron diffraction from the same sample (published in Ref. 20) shows 200/002 splitting and a (112) diffraction peak which confirms the crystalline phase to be tetragonal. The tetragonal phase was accompanied by an abrupt increase of the permittivity to 35. A slight reduction of dielectric constant is observed at higher temperature, which may be due to oxidation of the underlying metal electrode in residual oxygen. The leakage current distribution in crystalline tetragonal $\text{Hf}_{0.9}\text{Si}_{0.1}\text{O}_2$ is independent of area [Fig. 4(a)], which indicates that suppression of the tetragonal to monoclinic transformation does avoid formation of local defects. A 1000 times increase of leakage current is observed during the crystallization. Only a tenfold increase was observed during further increase of thermal budget to 1000 °C, suggesting crystallization to be the main driver in the leakage current degradation. The higher permittivity of the tetragonal phase allows physical thickening of the dielectric to mitigate the leakage current increase without losing capacitance. Figure 4(b) compares leakage current/CET scaling trends for amorphous HfO_2 (limited to 415 °C) and crystalline $\text{Hf}_{0.9}\text{Si}_{0.1}\text{O}_2$ (1000 °C). A flattening of the scaling trend is observed for crystalline HfSiO due to a change of the conduction mechanism from tunneling dominated to trap assisted. At a leakage current density of 10^{-7} A/cm^2 at 1 V, relevant to DRAM, a CET below 1.3 nm is achieved. This is comparable to the electrical properties of amorphous HfO_2 at low thermal budget. These results represent a significant improvement over recent metal-insulator-semiconductor and MIM (Refs. 5 and 21) results at high thermal budget.

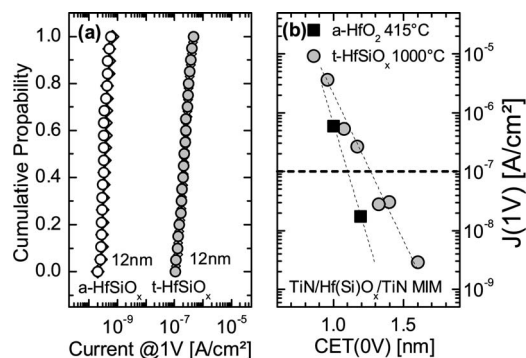


FIG. 4. (a) Statistics of leakage current density for amorphous and crystalline $Hf_{0.9}Si_{0.1}O_2$ of the same thickness for areas 1×10^{-4} and 2×10^{-2} cm^2 showing absence of local defects. (b) Leakage current vs CET relation for α - HfO_2 and t - $Hf_{0.9}Si_{0.1}O_2$ MIM capacitors.

In conclusion, excellent CET/leakage current characteristics were shown for amorphous HfO_2 . Crystallization of HfO_2 into the monoclinic phase leads to the formation of local defects with high leakage, severely limiting the applicability of m - HfO_2 as a dielectric. Stabilization of the tetragonal phase suppresses this defect mechanism while significantly enhancing the dielectric constant. The increased permittivity allows for a physically thicker film, compensating for the intrinsic leakage increase due to crystallization without capacitance loss. We suggest this strategy for HfO_2 based dielectrics in capacitors requiring high temperature stability.

Two of the authors (P.D.K. and B.H.L.) are IBM assignees.

¹J. Gavartin, D. M. Ramo, A. Shluger, G. Bersuker, and B. Lee, Appl. Phys. Lett. **89**, 082908 (2006).

²A. Kerber, E. Cartier, L. Pantisano, R. Degraeve, T. Kauerauf, Y. Kim, A. Hou, G. Groeseneken, H. E. Maes, and U. Schwalke, IEEE Electron Device Lett. **24**, 87 (2003).

- ³C. Cho, S. Song, S. Kim, S. Jang, S. Lee, H. Kim, Y. Sung, S. Jeon, G. Yeo, Y. Kim, Y. Kim, G. Jin, and K. Kim, Tech. Dig. VLSI Symp. **2005**, p. 36.
- ⁴P. D. Kirsch, M. A. Quevedo-Lopez, S. A. Krishnan, B. H. Lee, G. Pant, M. J. Kim, R. M. Wallace, and B. E. Gnade, Appl. Phys. Lett. **89**, 242909 (2006).
- ⁵W. Mueller, W. Bergner, E. Erben, T. Hecht, S. Jakschik, C. Kapteyn, A. Kersch, S. Kudelka, F. Lau, J. Luetzen, and A. Orth, Tech. Dig. - Int. Electron Devices Meet. **2005**, 347.
- ⁶G. Pant, A. Gnade, M. J. Kim, R. M. Wallace, B. E. Gnade, M. A. Quevedo-Lopez, and P. D. Kirsch, Appl. Phys. Lett. **88**, 032901 (2006).
- ⁷A. Navrotsky, J. Mater. Chem. **15**, 1883 (2005).
- ⁸J. Wang, H. P. Li, and R. Stevens, J. Mater. Sci. **27**, 5397 (1992).
- ⁹G.-M. Rignanese, X. Gonze, G. Jun, K. Cho, and A. Pasquarello, Phys. Rev. B **69**, 184301 (2004).
- ¹⁰X. Zhao and D. Vanderbilt, Phys. Rev. B **65**, 233106 (2002).
- ¹¹K. Tomida, K. Kita, and A. Toriumi, Appl. Phys. Lett. **89**, 142902 (2006).
- ¹²K. Kita, K. Kyuno, and A. Toriumi, Appl. Phys. Lett. **86**, 102906 (2005).
- ¹³E. Rauwel, C. Dubourdieu, B. Holländer, N. Rochat, F. Ducroquet, M. D. Rossell, G. V. Tendeloo, and B. Pellissier, Appl. Phys. Lett. **89**, 012902 (2006).
- ¹⁴Y. Senzaki, S. Park, H. Chatham, L. Bartholomew, and W. Nieveen, J. Vac. Sci. Technol. A **22**, 1175 (2004).
- ¹⁵J. Heitmann, A. Avellán, T. Böske, E. Erben, B. Hintze, S. Jakschik, S. Kudelka, and U. Schröder, ECS. Trans. **2**, 217 (2006).
- ¹⁶A. H. Heuer, M. Ruble, and D. B. Marshall, J. Am. Ceram. Soc. **73**, 1084 (1990).
- ¹⁷C. Zhao, V. Cosnier, P. J. Chen, O. Richard, G. Roebben, J. Maes, S. V. Elshocht, H. Bender, E. Young, O. V. D. Biest, M. Caymax, W. Vandervorst, S. De Gendt, and M. Heyns, Mater. Res. Soc. Symp. Proc. **745**, N1.5.1 (2003).
- ¹⁸D. A. Neumayer and E. Cartier, J. Appl. Phys. **90**, 1801 (2001).
- ¹⁹S. V. Ushakov, A. Navrotsky, Y. Yang, S. Stemmer, K. Kukli, M. Ritala, M. A. Leskel, P. Fejes, A. Demkov, C. Wang, B.-Y. Nguyen, D. Triyoso, and P. Tobin, Phys. Status Solidi B **241**, 2268 (2004).
- ²⁰T. S. Böske, S. Govindarajan, C. Fachmann, J. Heitmann, A. Avellan, U. Schröder, S. Kudelka, P. Kirsch, C. Krug, P. Y. Hung, J. Price, M. Quevedo-Lopez, G. Pant, B. E. Gnade, W. Krautschneider, B. H. Lee, and R. Jammy, Tech. Dig. - Int. Electron Devices Meet. **2006**, 255.
- ²¹T. Ando, N. Sato, S. Hiyama, T. Hirano, K. Nagaoka, H. Abe, A. Okuyama, H. Ugajin, K. Tai, S. Fujita, K. Watanabe, R. Katsumata, J. Idebuchi, T. Hasegawa, H. Iwamoto, and S. Kadomura, Jpn. J. Appl. Phys., Part 1 **45**, 3165 (2006).